3 Biotech (2019) 9:402
https://doi.org/10.1007/s13205-019-1947-6

ORIGINAL ARTICLE

Antibiofilm potential of Seabuckthorn silver nanoparticles (SBT@AgNPs) against *Pseudomonas aeruginosa*

Vijay Singh Gondil[1] · Thiyagarajan Kalaiyarasan[2] · Vijay K. Bharti[2] · Sanjay Chhibber[1]

Received: 17 June 2019 / Accepted: 10 October 2019 / Published online: 19 October 2019

Abstract

In era of antibiotic resistance, antibacterial silver nanoparticles are considered as potential alternative therapeutic agent to combat drug resistant pathogens. The aim of present study was to evaluate the antibacterial, antibiofilm and biocompatible potential of green synthesized Seabuckthorn silver nanoparticles (SBT@AgNPs). In the study, antibacterial efficiency of SBT@AgNPs was studied against *Pseudomonas aeruginosa*, *Klebsiella pneumoniae*, *Escherichia coli* and methicillin resistant *Staphylococcus aureus*. SBT@AgNPs were found to possess high antibacterial activity which was indicated in terms of low minimum inhibitory and bactericidal concentrations (2–4 µg/ml) obtained against test pathogens. Anti-biofilm activity of SBT@AgNPs on young as well as mature *P. aeruginosa* biofilms was also evaluated. SBT@AgNPs were able to eradicate the *P. aeruginosa* biofilms, which was further confirmed by field emission scanning electron microscopy and confocal laser scanning microscopy. Quorum sensing assay also revealed the quorum quenching activity of SBT@AgNPs. Biocompatibility and cytocompatibility results demonstrated SBT@AgNPs to exhibit first-rate non-toxicity as no membrane damage on RBCs or detrimental morphology variation was seen in human dermal fibroblast. LC–MS analysis was also carried out to analyze the potential antibacterial chemical compounds present in aqueous extract of Seabuckthorn leaves. To the best of our knowledge this is first study in which green synthesized silver nanoparticles were exploited to eradicate young as well as mature biofilms of *P. aeruginosa*. Results showed that SBT@AgNPs are highly antibacterial, antibiofilm, nontoxic in nature and consequently can aid in biomedical applications.

Keywords Seabuckthorn silver nanoparticles · Biofilms · *Pseudomonas aeruginosa* · Antibiotic resistance

Introduction

Pseudomonas aeruginosa has emerged as a potent pathogen during the last two decades due to its ability to cause a variety of infections that are encountered in our daily life. It is the second most common nosocomial infection involved in pneumonia, third most common organism isolated in both urinary tract infection (UTI) and surgical site infection (Richards et al. 1999). Most of the *P. aeruginosa* infections are established by means of their biofilm forming ability (Worthington et al. 2012). Biofilms are three dimensional complex of bacterial cells, extracellular DNA, proteins and polysaccharides and exhibit a significant difference in their physiology from planktonic cells (Costerton et al. 1995; Flemming et al. 2007; Kostakioti et al. 2013). As a result, biofilm increase the persistence of bacteria by decreasing their susceptibility to immune and inflammatory responses which in turn lower the clearance of bacteria from body (Hutchison and Govan 1999; Overhage et al. 2008). National Institutes of Health (NIH) reported that worldwide approx 80% bacterial infections are in form of biofilms and majority of them fail to respond to all available antibiotics and antimicrobial products/disinfectants (Overhage et al. 2008; Schaudinn et al. 2009). Biofilms are up to 1000-fold more resistant to conventional antibiotic treatment than planktonic

Vijay Singh Gondil and Thiyagarajan Kalaiyarasan: equal contribution.

Electronic supplementary material The online version of this article (https://doi.org/10.1007/s13205-019-1947-6) contains supplementary material, which is available to authorized users.

✉ Sanjay Chhibber
sanjaychhibber8@gmail.com

[1] Department of Microbiology, Basic Medical Sciences, Panjab University, Chandigarh 160014, India

[2] Defence Institute of High Altitude Research (DIHAR), DRDO, Leh-Ladakh, J&K 194101, India

bacteria. According to World Health Organization (WHO) *P. aeruginosa* is listed as second greatest threat to develop antibiotic resistance and is a matter of concern as it is equipped with a range of genetic factors that determine its virulence.

In an attempt to overcome the menace of drug resistance, scientists are globally paying attention to develop new alternatives antibiotics/antimicrobials that not only take care of resistance development but also reduce the usage of conventional antibiotics. Phages (Gondil and Chhibber 2018), therapeutic enzymes (Nelson et al. 2006; Chhibber et al. 2018; Liu et al. 2014), quorum sensing inhibitors (Hentzer et al. 2002), efflux pump inhibitors (Lamers et al. 2013), phytochemicals (Moreno et al. 2013), pigments (Gondil et al. 2017) and antibacterial metal nanoparticles (Kumar et al. 2017) are being explored for their antibacterial potential. Among them, silver nanoparticles have gained much attention because of their high antibacterial activity against drug resistant superbugs. Though, AgNPs can be synthesized by both chemically and biogenic route yet biological route for synthesis of AgNPs has received great attention due to its less toxicity towards mammalian cells. Biogenic methods, especially plant extracts based reduction is more viable because of its low cost, rapid preparation, normal physical conditions and easily scale up (Mittal et al. 2013). In this perspective, we previously reported Seabuckthorn (*Hippophae rhamnoides* L.) leaves extract mediated SBT@AgNPs synthesis and their longevity, antibacterial, antioxidant potential (Kalaiyarasan et al. 2017). We reported that SBT@AgNPs had antibacterial activity against variety of organisms but yet to know whether SBT@AgNPs can alter the virulence of an organism in terms of biofilm formation that in turn regulated through quorum sensing, made us plan this study. In present study antibiofilm and antiquorum potential of SBT@AgNPs against young and mature *P. aeruginosa* biofilms was investigated.

Materials and methods

All materials used in this study were procured from Sigma-Aldrich and microbial culture media are obtained from Himedia Laboratories Pvt. Ltd, Mumbai, India. In all the experiments, Millipore water (18.2 U) was used (Millipore Applied Systems, USA).

Bacterial strains and SBT@AgNPs

Standard strain of *K. pneumoniae* B5055, *P. aeruginosa* PAO1, *E. coli* 25922 and Methicillin resistant *S. aureus* 43300 used in present study, were available in our laboratory. Bacterial cultures were maintained on the nutrient agar slants throughout the course of study.

SBT@AgNPs synthesis and characterization

For the synthesis of SBT@AgNPs detailed procedure has been described earlier (Kalaiyarasan et al. 2017). Briefly, 2 mg of lyophilized Seabuckthorn leaf powder were added to a flask containing 100 ml of 1000 ppm $AgNO_3$ solution and stirrer for 15 min at 100 rpm. The mixture was incubated for 24 h at room temperature (away from light), and at the end of incubation synthesized SBT@AgNPs were collected by centrifugation at 10000 rpm for 20 min and washed thrice with distilled water and the pellet (i.e., SBT@AgNPs) was resuspended in milli-Q-water and dried at 50 °C in a hot air oven. The dried SBT@AgNPs were used for different analytical characterization such as UV–Vis spectrophotometer, TEM, Zeta/surface charges afterwards antibiofilm, antiquorum and toxicity studies performed.

Well diffusion assay

Well diffusion assay was performed to evaluate the antibacterial potential of SBT@AgNPs against a wide range of pathogens. Nutrient agar plates were prepared and 100 µl of log phase culture (10^5–10^6 CFU/ml) of *K. pneumoniae*, *P. aeruginosa*, *E. coli*, *and S. aureus* were spread plated on different plates. Plates were then punched with the help of 5 mm sterile gel puncher to form wells and 50 µl of SBT@AgNPs (1 mg/ml in sterile distilled water) was filled in each well. Afterwards, the plates were incubated at 37 °C overnight and next day, zone of inhibition was observed.

Minimum inhibitory concentration (MIC) and Minimum bactericidal concentration (MBC) determination

MIC and MBC of SBT@AgNPs against different bacterial strains was evaluated by broth dilution method as proposed by National Committee for Clinical Laboratory Standards (CLSI 2019). Briefly, wide range dilutions (1–128 µg/ml) of SBT@AgNPs were prepared and 100 µl of each dilution was incubated with 100 µl of log culture (10^5–10^6 CFU/ml) of *K. pneumoniae*, *P. aeruginosa*, *E. coli* and *S. aureus* in a 96 well microtitre plate for 18–24 h at 37 °C. Minimum dilution of SBT@AgNPs showing no visible turbidity in broth was termed as MIC of SBT@AgNPs against tested pathogen. For MBC, contents from each well were plated on separate nutrient agar plates and incubated overnight at 37 °C. Next day, lowest concentration of SBT@AgNPs showing no growth on nutrient agar plate was termed as MBC of SBT@AgNPs against tested pathogen.

Establishment and processing of *P. aeruginosa* biofilm

P. aeruginosa PAO1 biofilm was established in a 96-well microtiter plate up to 7 days as previously described by Wagner et al. (2007). Briefly, 100 µl of *P. aeruginosa* log culture (OD_{600} 0.5) was added into each well of a microtiter plate and incubated for 24 h at 37 °C. The well containing only a sterile nutrient broth served as sterility control. Every 24 h of incubation, broth containing planktonic cells was removed from the wells and wells were washed thrice with PBS (pH 7.4). Then, fresh sterile fresh nutrient broth was added into each well and further incubated at 37 °C. In order to achieve the biofilm, same procedure was followed up to 7th days. The biofilm formation was examined by using two different methods which includes, viable cell counting (quantitative method) and crystal violet staining (semi quantitative method) respectively. For viable cell counting after each 24 h, selected wells were aspirated to remove planktonic cells, washed thrice with PBS and scraped with the help of 5 mm sterile gel puncher in 100 µl of PBS. Appropriate dilution of scraped cells from each well were plated on nutrient agar plates and incubated overnight at 37 °C. For crystal violet staining, duplicate wells on each day were stained with 0.1% (w/v) of crystal violet stain for 10 min, gently washed with 200 µl of PBS and destained with 95% ethanol. Contents from each well were observed on ELISA reader (BIO RAD) at 595 nm.

Evaluate the effect of SBT@AgNPs on *P. aeruginosa* biofilm

Antibacterial efficacy of SBT@AgNps on *P. aeruginosa* biofilm was determined by using MIC and MBC concentrations. 200 µl of MIC and MBC concentrations of SBT@AgNps were added to selected test wells. In control wells, 200 µl of sterile water was added to well up to 7 days. Microtiter plate was again incubated at 37 °C for 6 h and at the end of incubation the contents from treated and control wells were processed to determine the viable count. The CV staining was also performed in order to determine the optical density of cells in the biofilm. Media from remaining wells was aspirated and replaced with fresh nutrient broth after PBS washing. The procedure was repeated daily up to 7th days. Biofilm eradication in treated wells was estimated in terms of bacterial count and CV staining as compared to control wells.

Field emission scanning electron microscope (FESEM) and compositional analysis of biofilm

For FESEM and compositional analysis of *P. aeruginosa* biofilm, biofilms were prepared on cover slips using batch culture model (Hughes et al. 1998). 500 µl of nutrient broth, 500 µl of bacterial culture of *P. aeruginosa* (OD_{600} 0.05) and a sterile cover slip was added to each well. Sterile broth was added to last well of each row and taken as sterility control. Microtitre plate was incubated at 37 °C for 7 days and media was replaced with sterile nutrient broth after washing with PBS on each day. To evaluate the antibiofilm efficacy of SBT@AgNps on peak day of biofilm, biofilm was treated with MIC and MBC concentration of SBT@AgNps. Microtitre plates were re-incubated at 37 °C for 6 h. The 4th (peak) day control and MBC treated biofilms were fixed with 2.5% gluteraldehyde, dehyrated and coated with ion sputter. Control and treated biofilms were subjected to FESEM (Hitachi SU8010) and energy dispersive X-ray spectroscopy (Brukner XFlash6130) to analyze the morphology and elemental composition of biofilm at SAIF-CIL, Panjab University, Chandigarh.

Confocal Laser Scanning Microscopy (CLSM) examination of biofilm

Biofilm was established on a coverslip as described in "Evaluate the effect of SBT@AgNPs on *P. aeruginosa* biofilm". On peak day, biofilm was treated with SBT@AgNps at MIC and MBC concentrations for 6 h at 37 °C. In case of control biofilm, no treatment was given and sterile water was added instead of SBT@AgNps. For confocal microscopy, coverslips from 4th day biofilm, were stained with fluorescent dyes (Propidium iodide red and SYTO9, Thermo scientific, USA) and observed under inverted confocal laser scanning microscope (SCLM, Nikon Ti Eclipse).

Anti-Quorum sensing inhibition assay

Anti-Quorum sensing inhibition activity of SBT@AgNPs was investigated by well diffusion assay. Briefly, about 40 µl of X-gal (20 mg/ml in dimethylformamide) was spread on Luria agar plates and allowed to dry for 5–10 min at room temperature. Then, about 100 µl of synthetic AHLs (*N*-3-oxo-dodecanoyl-L-homoserine lactone, 1 mg/ml) and *P. aeruginosa* extracted AHLs were applied on separate plates. For control plates, only X-gal were spreaded on the Luria agar plates without any AHLs. Plates were incubated for 30 min at room temperature for proper absorption. Subsequently, about 100 µl of *Agrobacterium tumefaciens* A136 was spread evenly on same plates and dried at room temperature for 10 min. Further, well in the center of each plate was loaded with 100 µl of SBT@AgNPs suspension and allowed to diffuse for 60 min. The plates were incubated at 30 °C for 48 h and after incubation, appearance of colorless zone was analyzed for inhibition of quorum sensing caused by SBT@AgNPs and compared the results with control.

Investigation of SBT@AgNPs biocompatibility

The hemolysis assay was performed with chicken whole blood as described by Kutwin et al. (2014) to evaluate the biocompatibility of Seabuckthorn aqueous extract containing silver nanoparticles. Briefly, heparinized blood collected from the slaughter house was incubated at 37 °C at 120 rpm with 8, 16, and 32 µg/ml SBT@AgNPs. Then, the blood was centrifuged at 1200 rpm for 10 min and supernatant collected. The amount of hemoglobin was estimated in the supernatant at 540 nm using a plate reader (Spectramax i3x, Molecular Devices, CA, USA). The sample incubated with Triton X-100 was served as a positive control and the sample with PBS buffer served as a negative control. The percentage of hemolysis was calculated using the formula described by Thiyagarajan et al. (2017). The structural damage of erythrocytes (RBCs) was analyzed by using upright light microscopes at 40 × (Leica Microsystems, Germany).

Cytotoxicity studies of SBT@AgNPs

For this study, human dermal fibroblast (with passage 12 ± 3), kindly gifted by Dr. Johnson, Center for Nanoscience and nanotechnology, Sathyabama Institute of Science and Technology, Chennai, Tamil Nadu, India was used. The cells were maintained in Dulbecco's modified eagles medium (DMEM, Sigma-Aldrich, MO), supplemented with 10% FBS (HiMedia Laboratories Pvt. Ltd.) and penicillin (100 U/ml), streptomycin (100 µg/ml) and amphotericin B (100 µg/ml) to confluency in T75 flask. The cells were maintained at 37 °C in a humidified chamber in presence of 5% CO_2 and 95% atmospheric air. The culture medium was changed every 2 days interval. The growth characteristics of cells were examined under light microscope. When the culture reached 90–95% confluence, the cells were then detached from the flask with 1–2 ml trypsin digestion (Invitrogen). Then, the cell suspension was transfered into 15 ml screw cap tube and centrifuged. After centrifugation the cell pellet was reconstituted with 10% FBS-supplemented with DMEM and cell morphology was visualized under microscope (EVOS FL Cell Imaging System).

SBT@AgNPs treatment

For cell viability, stock solution of SBT@AgNPs was prepared (1 mg/ml) in sterile distilled water and diluted to achieved the required concentration using cell culture media. Then, human dermal fibroblast were plated in 96-well plates (Nunc, Thermo Fisher Scientific, Denmark) and exposed to different concentration of SBT@AgNPs viz 8, 16, and 32 µg/ml. Cells were maintained in a humidified atmosphere at 37 °C in presence of 5% CO_2; At 24, 48 and 72 h of SBT@AgNPs exposure, the medium was removed from each well, replaced with a new medium and the plates were observed under a light microscope to detect morphological changes and photographed at each time interval (24, 48 and 72 h) (EVOS FL Cell Imaging System). Thereafter, MTT assay was performed at each time point (i.e., 24, 48 and 72 h), about 10 µl of MTT (5 mg/ml) was added to each well and plate was incubated for 4 h at 37 °C. The resulting formazan was dissolved in 100 µl of DMSO per well and absorbance was measured at 570 nm using a plate reader (EnSpire, Multimode Plate Reader) and the percentage (%) cell viability was calculated applying the following formula: (%) cell viability = Treated average OD/Control Average OD) × 100.

LC–MS analysis of SBT aqueous leaves extracts

In order to evaluate chemical compounds present in the extract from Seabuckthorn leaves the contents were evaluated using Shimadzu LCMS-8030, Japan attached with a triple quadrupole mass spectrometer. At the onset, 5 µl aqueous fractions were injected onto a C-18 column (4.6 25 cm, 5 lm; Phenomenex UK, Macclesfield, UK). The solvents used were 90% acetic acid–water (A) and 10% Acetonitrile (B). The elution gradient was isocratic 10% B for 5 min, 10–100% B over 20 min, 100% B for 6 min, and re-equilibration of the column, using a flow rate of 200 µl/min. Spectra were recorded in negative and positive ionization mode between m/z 50 and 1200.

Results

Synthesis and characterization of SBT@AgNPs

We have synthesized and characterized Seabuckthorn (*Hippophae rhamnoides* L.) leaves extract mediated AgNPs as described our earlier report (Kalaiyarasan et al. 2017). Transmission Electron Microscopy showed spherical structure of SBT@AgNPs with average particle size ranging from ~ 10 to 40 nm. Furthermore, zeta potentials of SBT@AgNPs was found with Negative ζ value − 29 ± 0.11 mV.

Well diffusion assay

Well diffusion assay revealed antibacterial nature of SBT@AgNps against both gram negative and gram positive pathogens. SBT@AgNps showed highest zone of inhibition against *P. aeruginosa* followed by *S. aureus* and *E. coli*. However, *K. pneumoniae* showed least sensitivity to SBT@AgNps as a narrow zone of inhibition was observed around the well containing SBT@AgNps (Fig. 1).

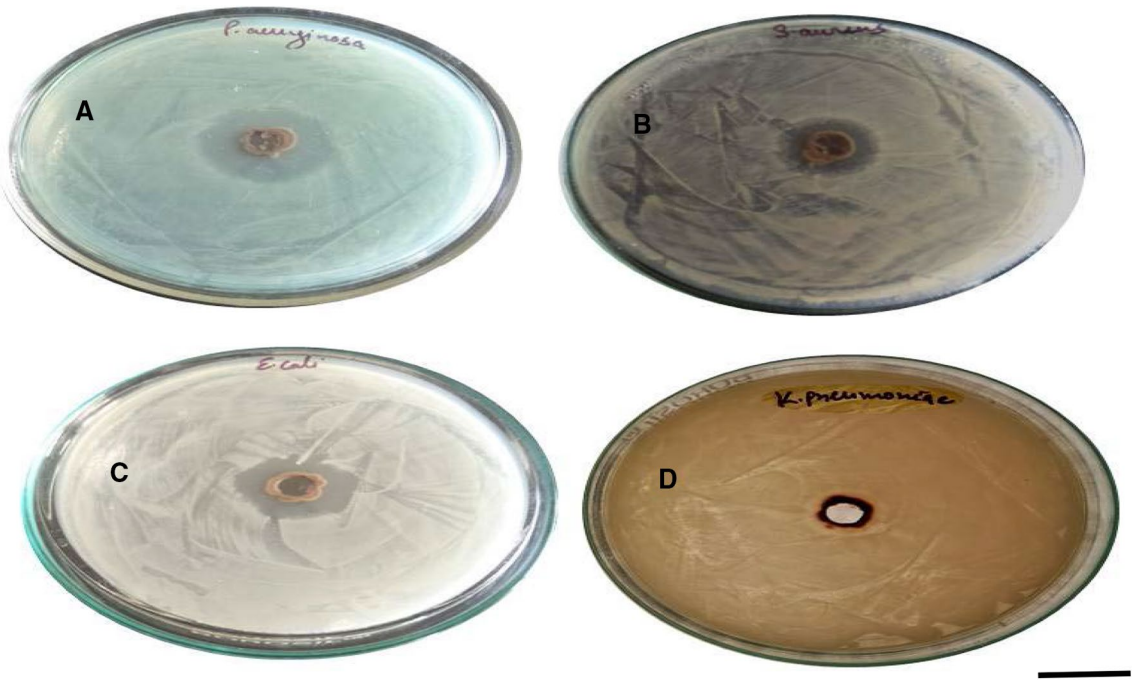

Fig. 1 Antibacterial activity of SBT@AgNps against *P. aeruginosa* (**a**), *S. aureus* (**b**), *E. coli* (**c**) and *K. pneumoniae* (**d**). Scale bar 10 mm

Table 1 MIC and MBC of SBT@AgNPs against a range of potential pathogens

Tested bacterial strains	MIC (µg/mL)	MBC (µg/mL)
P. aeruginosa PAO1	2	4
E. coli 25922	4	8
S. aureus 43300	4	8
K. pneumoniae B5055	8	16

MIC and MBC determination

SBT@AgNPs showed high antibacterial activity against test organisms and results are presented in Table 1. The MIC and MBC of SBT@AgNPs was lowest in case of *P. aeruginosa*, (i.e., 2 and 4 µg/ml each), it showed growth inhibition as well as bacterial killing. Significant MIC against other bacterial strains, *E. coli* (4 µg/ml) and *S. aureus* (4 µg/ml) was also observed. However, SBT@AgNPs restricted the growth of *K. pneumoniae* at higher concentration (8 µg/ml) of SBT@AgNPs as compared to other tested pathogens.

Kinetics of *P. aeruginosa* biofilm

P. aeruginosa biofilm was established, processed and observed for 7 day period. Viable cell counting method showed formation of biofilm with 4th day as peak day as maximum bacterial count of 10.84 ± 0.64 Log10 CFU/ml was observed. The results of Fig. 2 showed that after 4th day a gradual decrement in bacterial count was observed and continued up to 7th day. Similar results were also observed by semi quantitative crystal violet staining method. Crystal violet staining method also showed 4th day as peak day with maximum absorbance of 1.647 ± 0.079, after 4th day gradual decrease in absorbance was observed up to 7th day.

Biofilm eradication by SBT@AgNps

P. aeruginosa biofilm was established on a 96 well microtitre plate up to 7 days and treated with SBT@AgNps (MIC and MBC concentration) on each day. Cell viability results, as shown in Fig. 3 depicted significant reduction ($P < 0.01$) in bacterial load of young biofilm of *P. aeruginosa* following SBT@AgNps treatment. On peak day i.e. 4th day of biofilm, a significant reduction ($P < 0.01$) up to 7.63 ± 0.3 (MIC) and 5.27 ± 0.19 (MBC) logs was observed as compared to 11.42 ± 0.45 logs in control biofilm. Mature biofilm also showed susceptibility towards SBT@AgNps as significant bacterial reduction ($P < 0.01$) was observed in treated biofilms on day 5, 6 and 7 as compared to control untreated biofilm. Crystal violet staining was also performed and showed biofilm eradication upon treatment with SBT@AgNps (Supplementary data, S1).

FESEM and EDS analysis of biofilm

Biofilm of *P. aeruginosa* was established on a coverslip and analyzed by FESEM on peak day i.e. 4th day. FESEM

images revealed the 3D structure of intact bacterial cells along with matrix and water channels (Fig. 4a–c). Subsequently morphology of SBT@AgNPs treated (MIC and MBC concentrations) biofilm was analyzed by FESEM on 4th day treatment. The results shown the biofilm treated with MIC concentration intact 3D structure was disrupted into patches of matrix having embedded biofilm cells. In addition, SBT@AgNPs interacting bacterial cell membrane and disruption of bacterial wall also observed (Fig. 5a–c). However, MBC treated biofilm showed severe disruption of biofilm structure as compared to MIC treated biofilm ((Fig. 5d–f). The biofilm disruption resulted due to SBT@

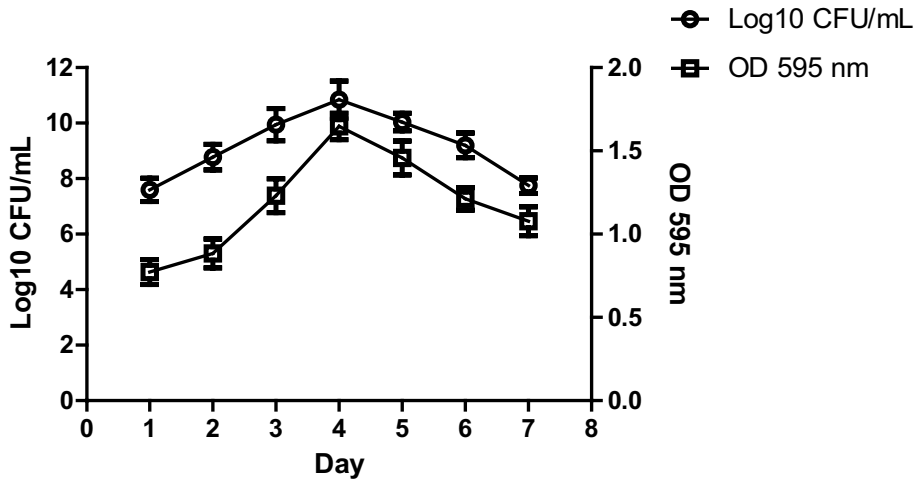

Fig. 2 Graph showing the kinetics of *P. aeruginosa* PAO1 biofilm as determined by viable cell count and crystal violet staining method up to 7 days. Bars showed the standard deviation in bacterial load and absorbance on each day

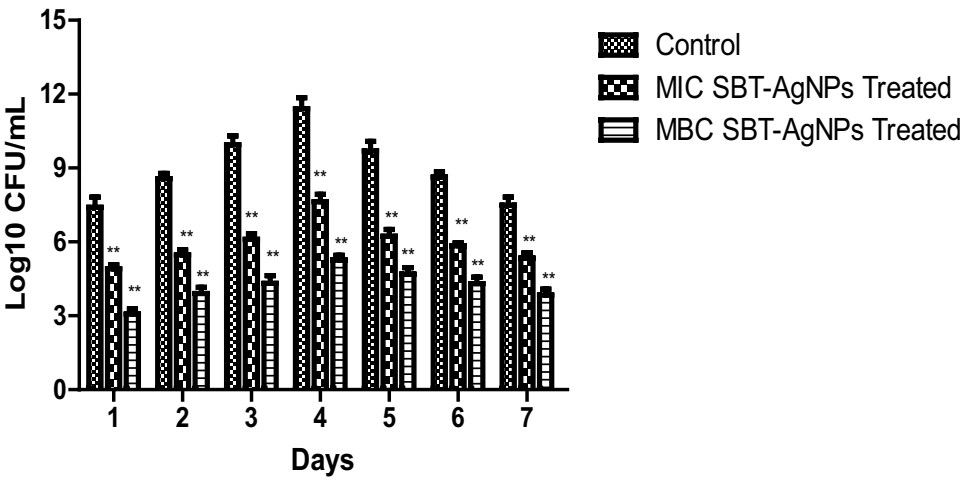

Fig. 3 Bacterial count in *P. aeruginosa* biofilm established for seven days and treated with SBT@AgNps on each day. Bars represents standard deviation and ** denotes *P* value ($P < 0.01$)

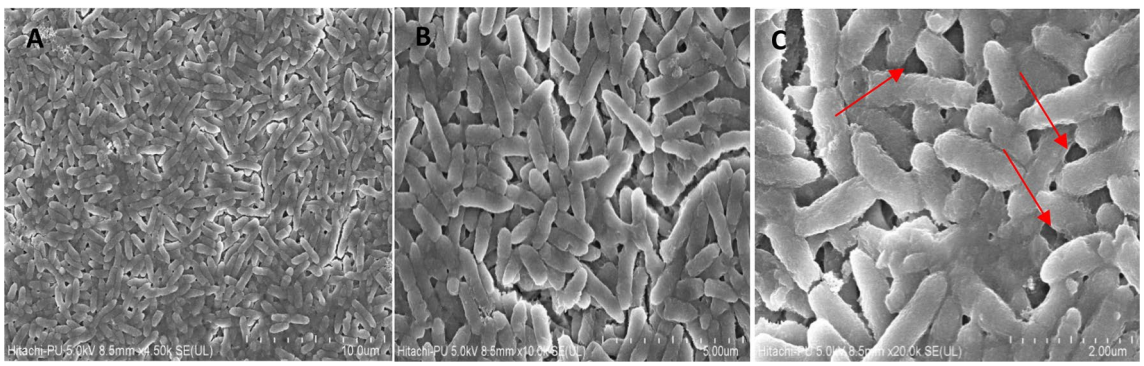

Fig. 4 FESEM images (**a**–**c**) of *P. aeruginosa* biofilm on 4th day at varying magnifications (×4–20 K magnifications). Water channels in biofilm matrix are depicted by arrows in image C

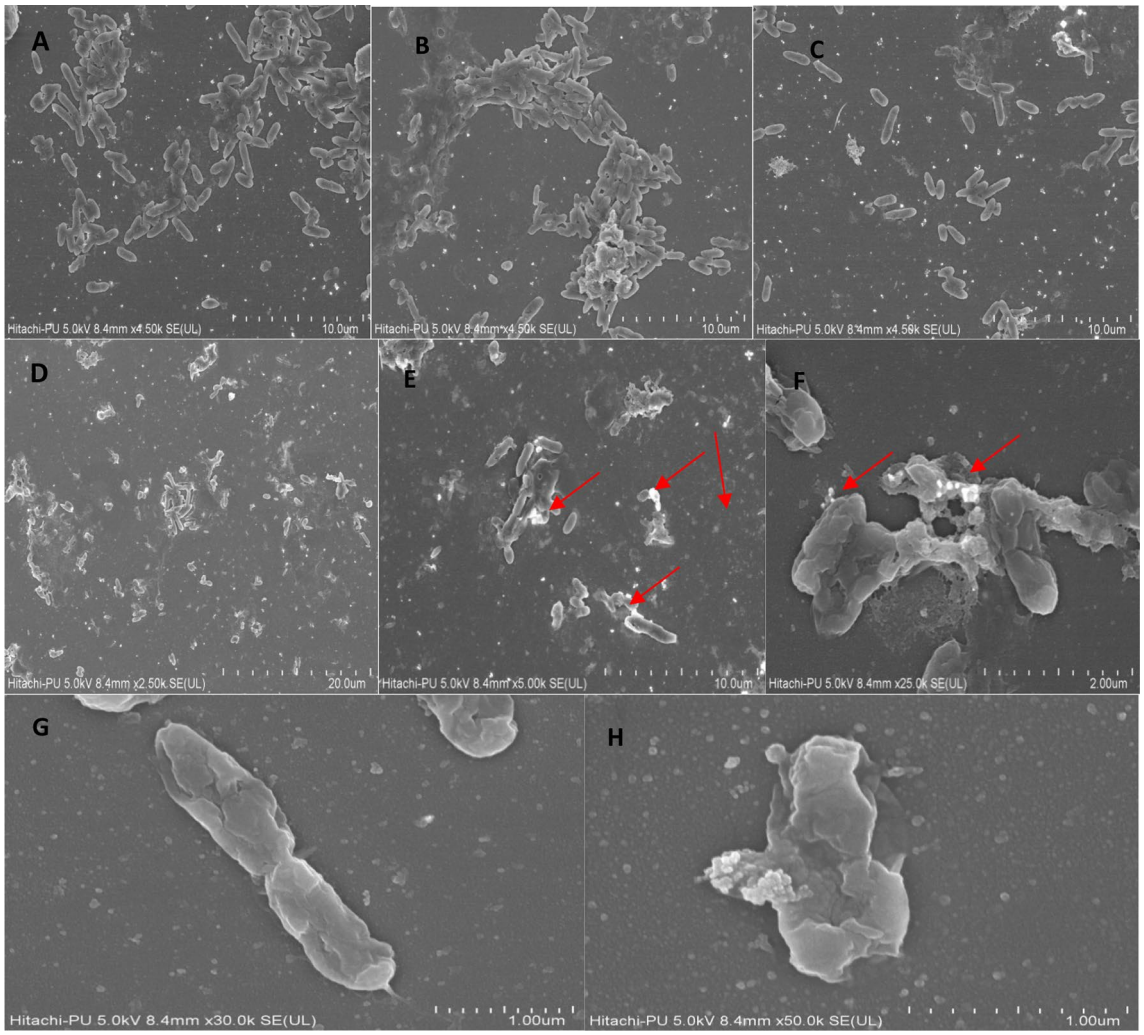

Fig. 5 FESEM images of MIC concentration (**a**–**c**) and MBC concentration (**d**–**f**) SBT@AgNps treated *P. aeruginosa* biofilm on 4th day at varying magnifications (×4.5–25 K magnifications). SBT@AgNps interacting with bacterial cells in biofilm matrix are depicted by arrows in image E and F. FESEM images of control and SBT@AgNps treated *P. aeruginosa* cells (**g**, **h**) at varying high magnifications (×30–50 K magnifications)

AgNps mediated bacterial killing and these nanoparticles can be seen interacting with bacterial cells (Fig. 5g, h). Concentration dependent biofilm eradication was observed upon treatment with SBT-AgNps. To confirm this hypothesis we have performed compositional analysis of control (untreated biofilm) by using EDS on 4th day (peak day of biofilm establishment). The obtained results showed the presence of oxygen, silicon, phosphorus, sulfur, chlorine, aluminum, potassium and carbon attributed to the phosphate buffer saline components and silicon and aluminum peaks can be attributed to glass coverslip and aluminum stub subsequently the percentage of different elements in untreated biofilm (Supplementary data, S2). Moreover, the biofilm treated with MBC concentration of SBT@AgNPs on 4th day shown additionally silver peaks at 0.2 and 3 keV along with peaks of other elements present which is present in the control untreated biofilm (Supplementary data, S3).

CLSM analysis of control and treated biofilm

Bacterial cell viability in 4 day old *P. aeruginosa* biofilm was analyzed by confocal laser scanning microscopy to determine the effect of nanoparticle treatment. Control biofilm contained majority of live cell in total cell population which showed the integrity of biofilm (Fig. 6a). In case of MIC treated biofilm a mixture of live and dead cells was seen, indicating the bactericidal action of SBT@AgNps (Fig. 6b). In MBC treated biofilm, dispersal of biofilm structure and high number of dead cells was observed as compared to live cells in total population,

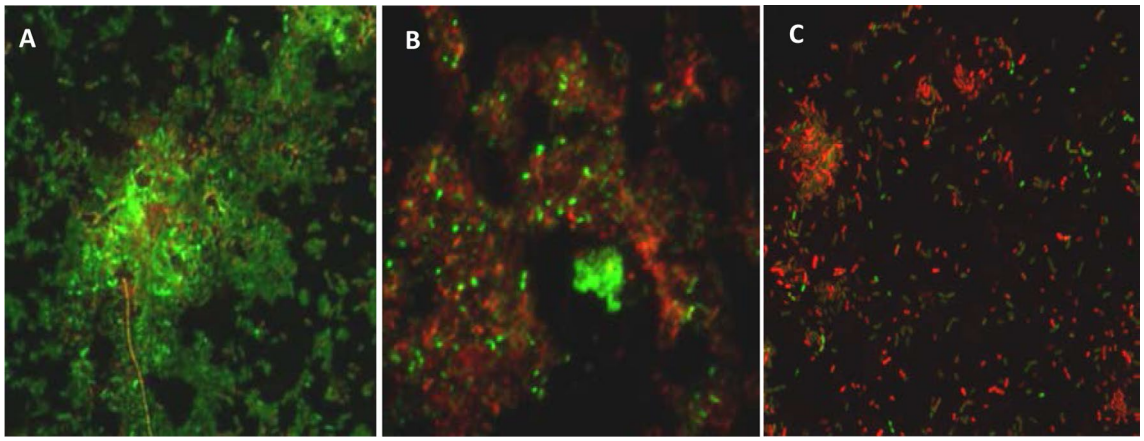

Fig. 6 *P. aeruginosa* PI and syto9 stained biofilm showing the effect of SBT@AgNps treatment under confocal microscope. Image **a** showing control untreated biofilm, **b** showing MIC SBT@AgNps treated biofilm and **c** showing MBC SBT@AgNps treated biofilm on peak 4th day (×400 magnification)

which confirmed the high efficacy of SBT@AgNps in eradicating bacterial biofilm (Fig. 6c).

Quorum sensing inhibition assay

Well diffusion assay revealed the antibacterial as well as anti-quorum behavior of SBT@AgNps. Synthetic AHLs and *P. aeruginosa* extract AHLs containing plates showed dual zone around the wells. First zone was ascribed to the antibacterial activity of the SBT@AgNps whereas second colorless zone of *A. tumefaciens* postulated the anti-quorum activity of SBT-AgNps. *P. aeruginosa* extracted AHLs and synthetic AHLs showed similar levels of SBT@AgNps mediated AHLs degradation as shown in Fig. 7.

Biocompatibility and cytotoxicity effects of SBT@AgNPs

Hemocompatiblity of SBT@AgNPs was evaluated on chicken whole blood on the basis of % hemolysis and membrane damage. The hemolysis and erythrocytes morphology following 1 h exposure of SBT@AgNPs to chicken whole blood was studied (Fig. 8). Maximum hemolysis (0.6%) was observed on highest dose of SBT@AgNPs (32 µg/ml). Microscopy of RBCs revealed normal morphology of RBCs with smooth surface and biconcave structure in control as well as SBT@AgNPs treated RBCs. These observations suggested that SBT@AgNPs did not cause significant hemolysis, structural damage to RBCs and exhibited well biocompatibility up to 32 µg/ml. Moreover, to investigate the cytotoxic properties of SBT@AgNPs, human dermal fibroblasts were incubated with SBT@AgNPs, analyzed by MTT assay and microscopic

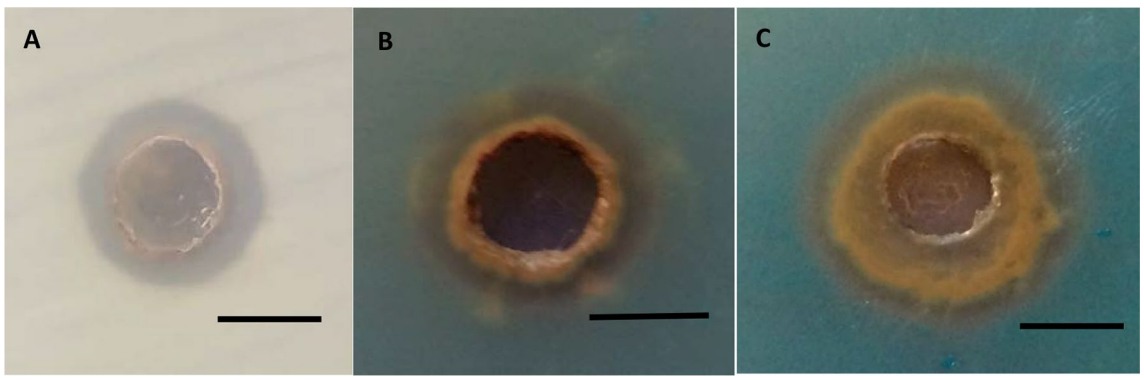

Fig. 7 Quorum inhibition assay of SBT@AgNps against Control without AHLs (**a**), synthetic AHLs (**b**) and *P. aeruginosa* extracted AHLs (**c**). Scale bar 5 mm

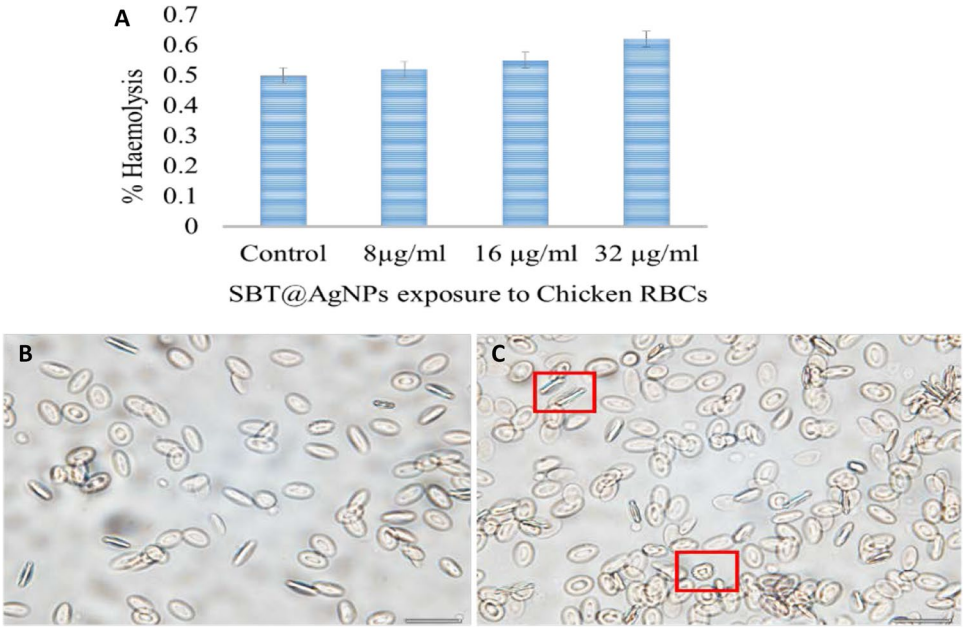

Fig. 8 Biocompatibility examination of SBT@AgNPs on chicken RBCs: **a** image showing % Haemolysis in chicken erythrocytes exposures to SBT@AgNPs in different concentration. **b**, **c** Morphology of chicken erythrocytes under upright light microscopy. Normal morphology of RBCs (**b**, control) with normal and smooth surface, **c** SBT@AgNPs treated with 32 µg/ml, RBCs showing insufficient number of swollen, indicating red box (×40 magnification)

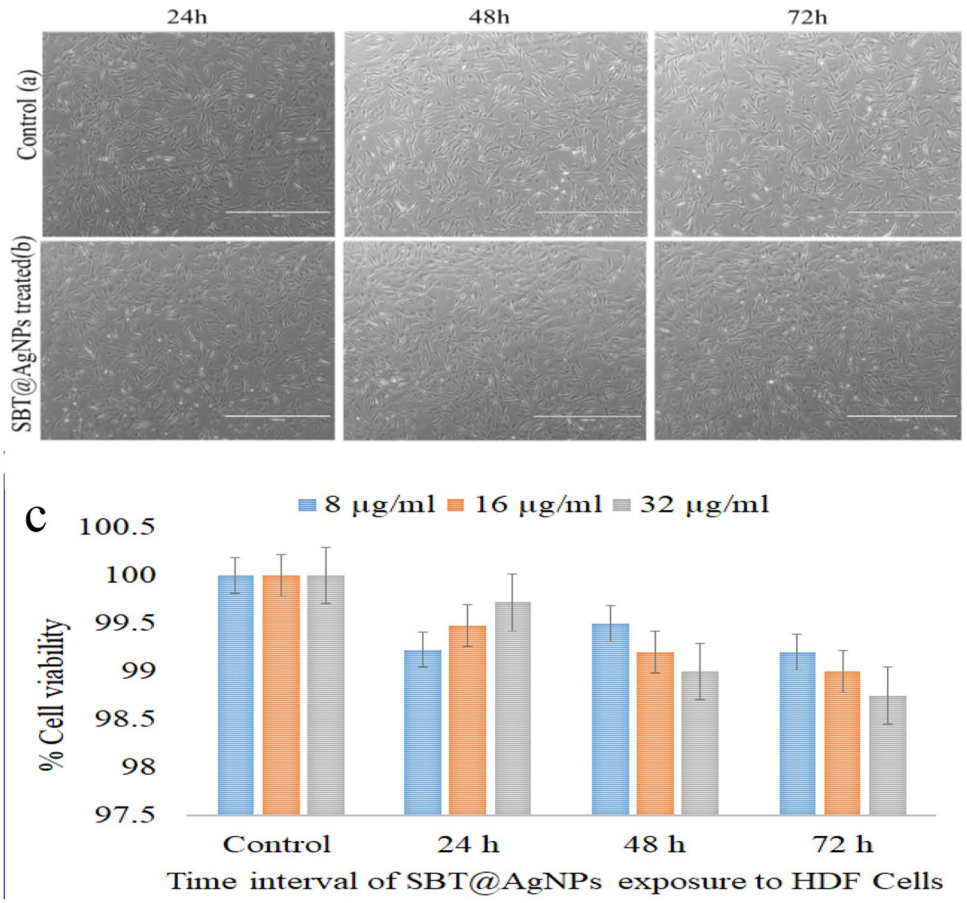

Fig. 9 Light microscopy images of cytotoxicity assays in human dermal fibroblast (HDF) at 24 to 72 h. Control (untreated) (**a**) and HDF treated with SBT@AgNPs 32 µg/ml concentration (**b**) MTT assay for metabolically active HDF upon exposure to SBT@AgNPs in different concentration at different time intervals (**c**) scale bar 1000 µm

examination (Fig. 9). Cell viability was found to be 99% at 48 h and 98.75% at 72 h of incubation upon exposure to SBT@AgNPs. The microscopic images did not show any distinct change in the cellular morphology after treatment with SBT@AgNPs. SBT@AgNPs showed reduced cytotoxicity of the nanomaterials synthesized by green

route confirming the improved biocompatibility of nanomaterials for biomedical applications.

LC–MS analysis of aqueous SBT leaves extract

LC–MS analysis of the aqueous extract from Seabuckthorn leaves enabled the identification of compounds (Fig. 10) belonging to different chemical families. The aqueous extract contained mainly phenolic compounds, Rutin, 3, 5, Dicaffeoylquinic acid and myricetin 3-O-glucoside. To best of our knowledge, 3, 5, Dicaffeoylquinic acid and myricetin 3-O-glucoside were identified for the first time in aqueous extract from Seabuckthorn leaves.

Discussion

Biogenic synthesis of AgNPs using medicinal plant extracts has conquered attention among the scientists in recent years because of their environment friendly nontoxic nature. A number of medicinal plants has been explored for AgNPs synthesis namely *Eleutherococcus senticosus, Rhynchosia suaveolens*, *Amaranthus retroflexus*, *Passiflora foetida* (Bahrami-Teimoori et al. 2017; Lade and Patil 2017; Bethu et al. 2018; Kim et al. 2018). Green synthesized AgNPs exhibits higher antibacterial as well as anticancer activity as compared to chemically synthesized silver nanoparticles (Kalaiyarasan et al. 2017). In a recent study by Kalaiyarasan et al. (2017), Seabuckthorn extract was used to synthesize silver nanoparticles, which were found to be highly stable for a year and also exerted antibacterial as well as antioxidant activity, supports the biological applications of synthesized nanomaterial.

In this regards, the present study SBT@AgNPs, were further explored for their antibacterial as well as antibiofilm activity. In initial attempts, antibacterial activity of SBT@AgNPs was accessed by well diffusion assay and MIC and MBC was determined against different well-established pathogens. SBT@AgNPs exhibited highest antibacterial activity against *P. aeruginosa* followed by *E. coli, S. aureus* and *K. pneumoniae*. High antibacterial activity of SBT@AgNPs can be correlated with reactive oxygen species

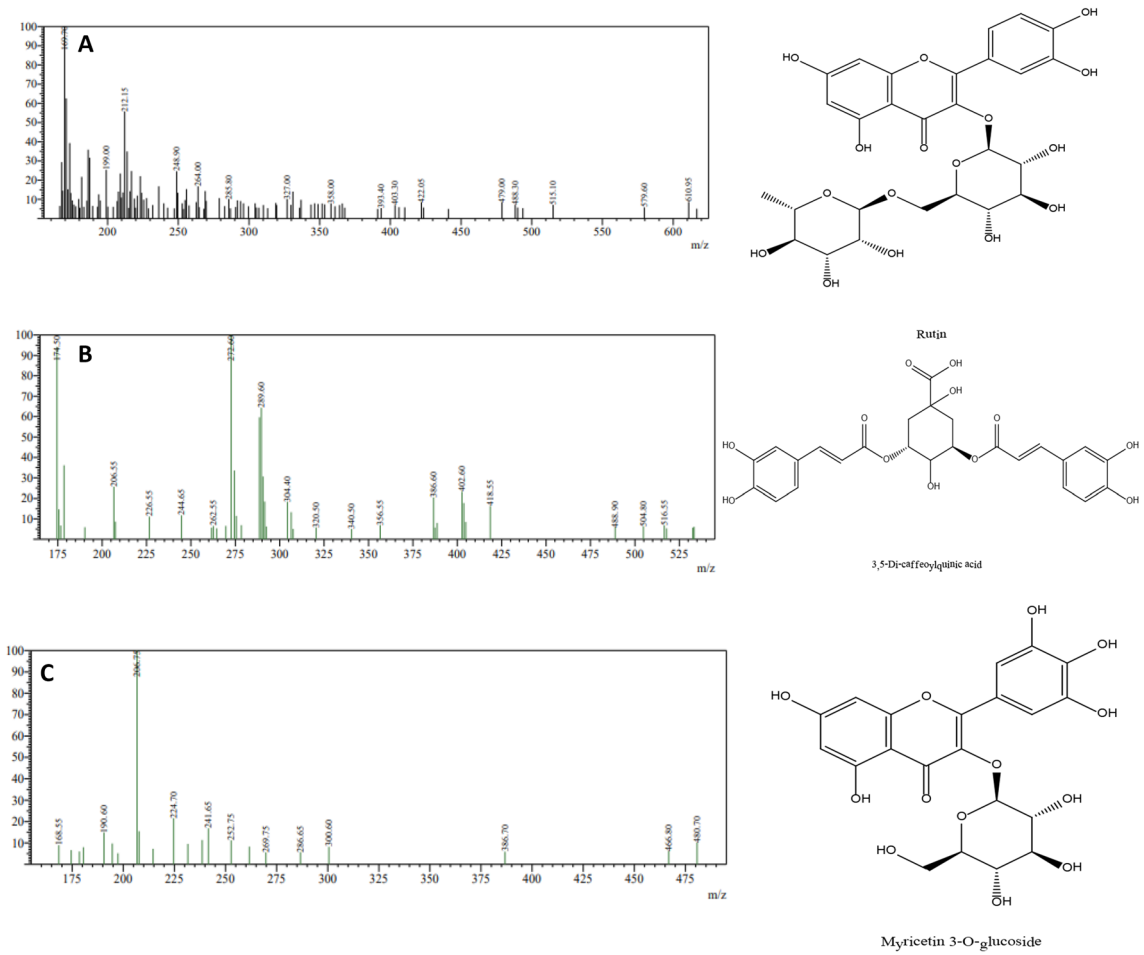

Fig. 10 Identification of the principal compounds in aqueous Seabuckthorn leaves extracts by LC–MS

generation and membrane damage as suggested in earlier studies (Kora and Arunachalam 2011; Kalaiyarasan et al. 2017). The low MIC and MBC of SBT@AgNps against potent pathogens eliminates the need of co-therapy with available conventional antibiotics. Moreover, SBT@AgNPs showed higher degree of susceptibility to *P. aeruginosa* as compared to other tested pathogens used in this study. In general, *P. aeruginosa*, is capable of forming biofilms which are tough to eradicate with available conventional antibiotics and extracellular matrix of biofilm presents resistance to environmental factors and antibiotics (Otto 2008; Gupta et al. 2016). With this, SBT@AgNPs were further explored for antibiofilm activity against *P. aeruginosa*. *P. aeruginosa* biofilm was established for 7 days. *P. aeruginosa* biofilm showed its peak count on 4th day and gradual decrease was observed thereafter. Harjai et al. (2014) also showed 4th day as a peak day for biofilm formation by *P. aeruginosa,* thus corroborating our findings. Established *P. aeruginosa* biofilms were treated with MIC and MBC concentrations of SBT@AgNps for 7 days and significant decrement in bacterial count was observed in treated biofilms as compared to control untreated biofilm over a seven day period. Crystal violet staining also confirmed the results of viable cell count and showed high reduction in optical density in MIC and MBC treated group on each day. In earlier studies green synthesized nanoparticles from medicinal plants have been used for eradication of S. *aureus*, *P. aeruginosa* and *E. coli* biofilms on young biofilms grown for 12–24 h (Bharathi et al. 2018; Singh et al. 2018) but there is no report where efficacy of these nanoparticles has been evaluated against mature biofilms. This is the first report where young and mature biofilms were tested for their susceptibility towards green synthesized nanoparticles.

Generally, antibacterial efficacy of any antibacterial agent is dependent on the age of biofilm (Sedlacek and Walker 2007; Ito et al. 2009). In mature biofilms are tough to eradicate owing to accumulation of extracellular matrix and altered cellular metabolic activity (Rani et al. 2007). On peak day, mature *P. aeruginosa,* control, MIC and MBC treated biofilms were observed by FESEM and EDS. FESEM analysis revealed the antibiofilm activity of SBT@AgNPs as disruption of biofilm was observed in both cases i.e., MIC and MBC treated biofilms as compared to control biofilm. Chhibber et al. (2017) also reported similar results in mature biofilm of *K. pneumoniae* was eradicated using Histidine capped silver nanoparticles. In our study, cell membrane destruction was seen in SBT@AgNPs treated biofilms under electron microscopy, which possibly describe the antimicrobial mechanism of SBT@AgNPs, additionally energy dispersive spectroscopy revealed the elemental composition of control and MBC treated biofilm, presence of silver in treated biofilm validated the silver nanoparticle mediated disruption of biofilm. Confocal laser scanning microscopy is a non-destructive method to study the structure as well as viability of biofilms (Psaltis et al. 2007). To validate our findings, control and treated biofilms were stained with Syto9 and Propidium iodide on peak day of biofilm formation. The results of confocal microscopy clearly showed high bacterial cell killing and membrane destruction in MIC and MBC treated biofilms as compared to control biofilms.

Cell to cell communication known as quorum sensing plays a vital role in *P. aeruginosa* biofilm formation (De Kievit 2009). In the present study we observed anti-quorum sensing activity of SBT@AgNps when tested in vitro. This additional advantage might help nanostructure in making an impact on biofilm at initial stage itself. It is therefore speculated that both anti-bacterial and anti-biofilm activities of SBT@AgNps will help in destroying the biofilm of *P. aeruginosa* in vivo as well. Shah et al. (2019) also showed antibiofilm and anti-quorum sensing activity of *Piper-betle* AgNPs against *P. aeruginosa* biofilms, supports present findings. Antiquorum sensing activity of SBT@AgNPs can be hypothesized as one of the major factors in eradicating bacterial biofilm by blocking cell to cell communication (Singh et al. 2013). Hemcompatibility and cell viability studies of SBT@AgNPs showed the biocompatible as well as cytocompatible nature of these biogenic synthesized nanostructures, supports their use in biomedical applications. LC–MS analysis of the aqueous extract from Seabuckthorn leaves showed the presence of phenolic compounds namely Rutin, 3, 5, Dicaffeoylquinic acid and myricetin 3-O-glucoside which is the possible reason for high antibacterial activity of SBT@AgNPs. On the contrary, N. K. Upadhyay et al. (2010) analyzed the aqueous extract of same plant using RP-HPLC and reported presence of quercetin-3-O-galcoside and quercetin-3-O-glucoside, indicating aqueous extract of Seabuckthorn is a rich source of a number of phenolic compounds and future studies may be devoted to their purification and identification of existing chemical compounds using other techniques. Since *P. aeruginosa* is a nosocomial pathogen generally associated with wound and burn infection, these nanoparticles at a very low dose will help in controlling the infection in hospital settings itself. This information will certainly help the scientists to evolve new anti-bacterial strategies in the light of increasing drug resistance in *P. aeruginosa*, especially in disruption of biofilm in comparison to planktonic cells.

Conclusion

In conclusion, SBT@AgNPs can be used for eradication of young as well as mature biofilms of *P. aeruginosa.* SBT@AgNPs showed excellent anti-quorum sensing ability, which may be helpful in controlling bacterial infection at initial

stages by blocking bacterial communication. SBT@AgNPs exhibited high biocompatibility on chicken blood and cytocompatibility on human dermal fibroblast at a concentration three times higher than MBC concentration. The present study proposes SBT@AgNPs as new alternative antimicrobial agent against drug resistant pathogens. However, future studies must be conducted to explore the in vivo potential of SBT@AgNPs.

Acknowledgements Mr. Vijay Singh Gondil is highly grateful to University Grants Commission (UGC), New Delhi, India for financial assistance in form of JRF/SRF. Kalaiyarasan and Vijay K Bharti are thankful to Defence Research and Developmental Organization (DRDO), New Delhi, India, for financial support, and Dr. Johnson, Center for Nanoscience and nanotechnology, Sathyabama Institute of Science and Technology, Chennai, Tamil Nadu, India, for providing cell culture facility to carry out cytotoxicity studies. The authors duly acknowledge Prof. Kusum Harjai, Ms. Surekha, Department of Microbiology, Panjab University, Chandigarh for quorum sensing studies, DST PURSE Project Implementation Group, Mangalore University, Karnataka, India for LC–MS facility, and Dr. Garima for help during results analysis, SAIF-CIL, Panjab University, Chandigarh for FESEM and EDS facility.

Funding The authors have no funding to report.

Compliance with ethical standards

Conflict of interest Authors declare no conflict(s) of interest.

References

Bahrami-Teimoori B, Nikparast Y, Hojatianfar M, Akhlaghi M, Ghorbani R, Pourianfar HR (2017) Characterisation and antifungal activity of silver nanoparticles biologically synthesised by Amaranthus retroflexus leaf extract. J Exp Nanosci 12(1):129–139

Bethu MS, Netala VR, Domdi L, Tartte V, Janapala VR (2018) Potential anticancer activity of biogenic silver nanoparticles using leaf extract of *Rhynchosia suaveolens*: an insight into the mechanism. Artif Cells Nanomed Biotechnol 46(sup1):104–114

Bharathi D, Vasantharaj S, Bhuvaneshwari V (2018) Green synthesis of silver nanoparticles using *Cordia dichotoma* fruit extract and its enhanced antibacterial, anti-biofilm and photo catalytic activity. Mater Res Express 5(5):055404

Chhibber S, Gondil VS, Sharma S, Kumar M, Wangoo N, Sharma RK (2017) A novel approach for combating a pneumoniae biofilm using histidine functionalized silver nanoparticles. Front Microbiol 8:1104

Chhibber S, Gondil VS, Kaur J (2018) Isolation, characterization, statistical optimization, and application of a novel broad-spectrum capsular depolymerase against *Klebsiella pneumoniae* from *Bacillus siamensis* SCVJ30. BBRJ 2(2):125

CLSI Performance Standards for Antimicrobial Susceptibility Testing (2019) 29 edition, CLSI supplement M 100. Clinical Laboratory Standards institute, Wayne

Costerton JW, Lewandowski Z, Caldwell DE, Korber DR, Lappin-Scott HM (1995) Microbial biofilms. Annu Rev Microbiol 49(1):711–745

De Kievit TR (2009) Quorum sensing in *Pseudomonas aeruginosa* biofilms. Environ Microbiol 11(2):279–288

Flemming HC, Neu TR, Wozniak DJ (2007) The EPS matrix: the "house of biofilm cells". J Bacteriol 189(22):7945–7947

Gondil VS, Chhibber S (2018) Exploring potential of phage therapy for tuberculosis using model organism. Biomed Biotechnol Res J 2:9–15

Gondil VS, Asif M, Bhalla TC (2017) Optimization of physicochemical parameters influencing the production of prodigiosin from Serratia nematodiphila RL2 and exploring its antibacterial activity. 3 Biotech 7(5):338

Gupta P, Chhibber S, Harjai K (2016) Subinhibitory concentration of ciprofloxacin targets quorum sensing system of *Pseudomonas aeruginosa* causing inhibition of biofilm formation & reduction of virulence. Indian J Med Res 143(5):643

Harjai K, Gupta RK, Sehgal H (2014) Attenuation of quorum sensing controlled virulence of *Pseudomonas aeruginosa* by cranberry. Indian J Med Res 139(3):446

Hentzer M, Riedel K, Rasmussen TB, Heydorn A, Andersen JB, Parsek MR, Rice SA, Eberl L, Molin S, Høiby N, Kjelleberg S (2002) Inhibition of quorum sensing in *Pseudomonas aeruginosa* biofilm bacteria by a halogenated furanone compound. Microbiology 148(1):87–102

Hughes KA, Sutherland IW, Jones MV (1998) Biofilm susceptibility to bacteriophage attack: the role of phage-borne polysaccharide depolymerase. Microbiology 144(11):3039–3047

Hutchison ML, Govan JR (1999) Pathogenicity of microbes associated with cystic fibrosis. Microbes Infect 1(12):1005–1406

Ito A, Taniuchi A, May T, Kawata K, Okabe S (2009) Increased antibiotic resistance of Escherichia coli in mature biofilms. Appl Environ Microbiol 75(12):4093–4100

Kalaiyarasan T, Bharti VK, Chaurasia OP (2017) One pot green preparation of Seabuckthorn silver nanoparticles (SBT@ AgNPs) featuring high stability and longevity, antibacterial, antioxidant potential: a nano disinfectant future perspective. RSC Adv 7(81):51130–51141

Kim CG, Castro-Aceituno V, Abbai R, Lee HA, Simu SY, Han Y, Hurh J, Kim YJ, Yang DC (2018) Caspase-3/MAPK pathways as main regulators of the apoptotic effect of the phyto-mediated synthesized silver nanoparticle from dried stem of *Eleutherococcus senticosus* in human cancer cells. Biomed Pharmacother 99:128–133

Kora AJ, Arunachalam J (2011) Assessment of antibacterial activity of silver nanoparticles on *Pseudomonas aeruginosa* and its mechanism of action. World J Microbiol Biotechnol 27(5):1209–1216

Kostakioti M, Hadjifrangiskou M, Hultgren SJ (2013) Bacterial biofilms: development, dispersal, and therapeutic strategies in the dawn of the postantibiotic era. Cold Spring Harbor Perspect Med 3(4):a010306

Kumar M, Bala R, Gondil VS, Pandey SK, Chhibber S, Jain DV, Sharma RK, Wangoo N (2017) Combating food pathogens using sodium benzoate functionalized silver nanoparticles: synthesis, characterization and antimicrobial evaluation. J Mater Sci 52(14):8568–8575

Kutwin M, Sawosz E, Jaworski S, Kurantowicz N, Strojny B, Chwalibog A (2014) Structural damage of chicken red blood cells exposed to platinum nanoparticles and cisplatin. Nanoscale Res Lett 9(1):257

Lade BD, Patil AS (2017) Silver nano fabrication using leaf disc of *Passiflora foetida* Linn. Appl Nanosci 7(5):181–192

Lamers RP, Cavallari JF, Burrows LL (2013) The efflux inhibitor phenylalanine-arginine beta-naphthylamide (PAβN) permeabilizes the outer membrane of gram-negative bacteria. PLoS One 8(3):e60666

Liu X, Tang Bo, Qiuya Gu, Xiaobin Yu (2014) Elimination of the formation of biofilm in industrial pipes using enzyme cleaning technique. MethodsX 1:130–136

Mittal AK, Chisti Y, Banerjee UC (2013) Synthesis of metallic nanoparticles using plant extracts. Biotechnol Adv 31(2):346–356

Moreno H, Paulo R, da Costa-Issa F, Rajca-Ferreira AK, Pereira MA, Kaneko TM (2013) Native Brazilian plants against nosocomial infections: a critical review on their potential and the antimicrobial methodology. Curr Top Med Chem 13(24):3040–3078

Nelson D, Schuch R, Chahales P, Zhu S, Fischetti VA (2006) PlyC: a multimeric bacteriophage lysin. Proc Natl Acad Sci 103(28):10765–10770

Otto M (2008) Staphylococcal biofilms. Bacterial biofilms. Springer, Berlin, pp 207–228

Overhage J, Campisano A, Bains M, Torfs EC, Rehm BH, Hancock RE (2008) Human host defense peptide LL-37 prevents bacterial biofilm formation. Infect Immun 76(9):4176–4182

Psaltis AJ, Ha KR, Beule AG, Tan LW, Wormald PJ (2007) Confocal scanning laser microscopy evidence of biofilms in patients with chronic rhinosinusitis. Laryngoscope 117(7):1302–1306

Rani SA, Pitts B, Beyenal H, Veluchamy RA, Lewandowski Z, Davison WM, Buckingham-Meyer K, Stewart PS (2007) Spatial patterns of DNA replication, protein synthesis, and oxygen concentration within bacterial biofilms reveal diverse physiological states. J Bacteriol 189(11):4223–4233

Richards MJ, Edwards JR, Culver DH, Gaynes RP (1999) Nosocomial infections in medical intensive care units in the United States. National Nosocomial Infections Surveillance System. Critical Care Medicine 27(5):887–892

Schaudinn C, Gorur A, Keller D, Sedghizadeh PP, Costerton JW (2009) Periodontitis: an archetypical biofilm disease. J Am Dent Assoc 140(8):978–986

Sedlacek MJ, Walker C (2007) Antibiotic resistance in an in vitro subgingival biofilm model. Oral Microbiol Immunol 22(5):333–339

Shah S, Gaikwad S, Nagar S, Kulshrestha S, Vaidya V, Nawani N, Pawar S (2019) Biofilm inhibition and anti-quorum sensing activity of phytosynthesized silver nanoparticles against the nosocomial pathogen *Pseudomonas aeruginosa*. Biofouling 35:1–6

Singh VK, Kavita K, Prabhakaran R, Jha B (2013) Cis-9-octadecenoic acid from the rhizospheric bacterium *Stenotrophomonas maltophilia* BJ01 shows quorum quenching and anti-biofilm activities. Biofouling 29(7):855–867

Singh P, Pandit S, Garnæs J, Tunjic S, Mokkapati VR, Sultan A, Thygesen A, Mackevica A, Mateiu RV, Daugaard AE, Baun A (2018) Green synthesis of gold and silver nanoparticles from *Cannabis sativa* (industrial hemp) and their capacity for biofilm inhibition. Int J Nanomed 13:3571

Thiyagarajan K, Bharti VK, Tyagi S, Tyagi PK, Ahuja A, Kumar K, Raj T, Kumar B (2018) Synthesis of non-toxic, biocompatible, and colloidal stable silver nanoparticle using egg-white protein as capping and reducing agents for sustainable antibacterial application. RSC Adv 8(41):23213–23229

Upadhyay NK, Kumar MY, Gupta A (2010) Antioxidant, cytoprotective and antibacterial effects of Sea buckthorn (*Hippophae rhamnoides* L.) leaves. Food Chem Toxicol 48(12):3443–3448

Wagner VE, Li LL, Isabella VM, Iglewski BH (2007) Analysis of the hierarchy of quorum-sensing regulation in *Pseudomonas aeruginosa*. Anal Bioanal Chem 387(2):469–479

Worthington RJ, Richards JJ, Melander C (2012) Small molecule control of bacterial biofilms. Org Biomol Chem 10:7457–7474